Quasi-static three point bending LS-DYNA analyses with MAT_CDPM (MAT_273) using tetra- and hexahedral meshes

Peter Grassl
School of Engineering, University of Glasgow, Glasgow, UK
Email: peter.grassl@glasgow.ac.uk

Last updated: 10 November 2017

1 Introduction

This document describes the results obtained from a set of three point bending analyses with Release 9.0.1 of LS-DYNA using MAT_CDPM (MAT_273). Tetra- and hexahedral meshes are used. MAT_CDPM (MAT_273) is based on work published in Grassl and Jirásek (2006); Grassl et al. (2013, 2011). The aim of these analyses is to demonstrate that the response obtained with MAT_CDPM for tensile failure of plain concrete is independent of the mesh size. More information on MAT_CDPM in LS-DYNA can be be found on: http://petergrassl.com/Research/DamagePlasticity/CDPMLSDYNA/index.html

2 Three point bending test with explicit and implicit LS-DYNA using tetra- and hexahedral meshes

The geometry and loading setup shown in Figure 1 is chosen according the experiment reported in Kormeling and Reinhardt (1982). In the experiments, the out-of-plane thickness was 100 mm.

The first set of analyses consisted of a three point bending test with coarse, medium and fine tetrahedral meshes. The LS-DYNA input files for these analyses are located

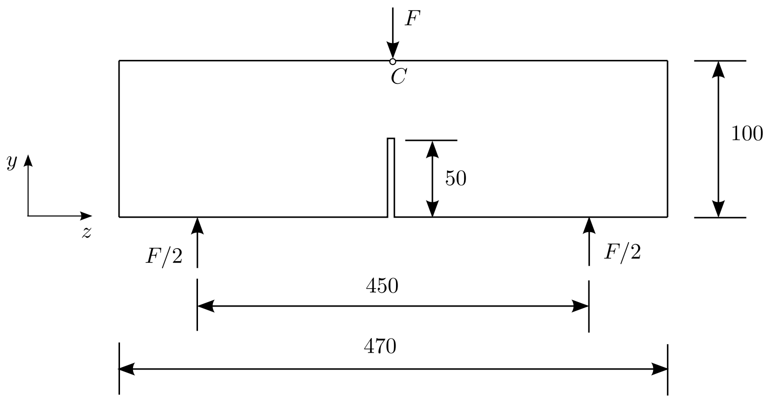

Figure 1: Three point bending test: Geometry and loading setup. The notch thickness is 5 mm.

```
*MAT_CDPM
$---+----1----+----2----+----3----+----4----+----5----+----6----+----7----+----8
$        |         |         |         |         |         |         |         |
$      MID       RHO         E        PR       ECC       QH0        FT        FC
         1    2.30E3     20.E9                                   2.4e6    24.e6
$        |         |         |         |         |         |         |         |
$       HP        AH        BH        CH        DH        AS        DF       FC0
      0.01                                                10
$        |         |         |         |         |         |         |         |
$     TYPE        BS        WF       WF1       FT1    STRFLG   FAILFLG       EFC
         1            185.1e-6
```

Figure 2: Input card for the three-point bending test.

in the folders TetraCoarse, TetraMedium and TetraFine. The meshes were generated with T3D (Rypl (1998)) according to the input files located in TetraMesh. The out-of-plane thickness for these meshes was selected to be 10 mm to reduce the required computational time compared. To be able to compare later the load-displacement curves with the experimental results, all the load values are multiplied by a factor of 10 to take into account the effect of reducing the out-of plane thickness of the specimens in the analyses. The input parameters were chosen according to the analyses carried out in Grassl et al. (2013). The input card for MAT_CDPM is shown in Figure 2.

The three meshes are shown in Figure 3. The load-displacement curves for the three explicit analyses are shown in Figure 4. For this quasi-static loading scenario, the explicit

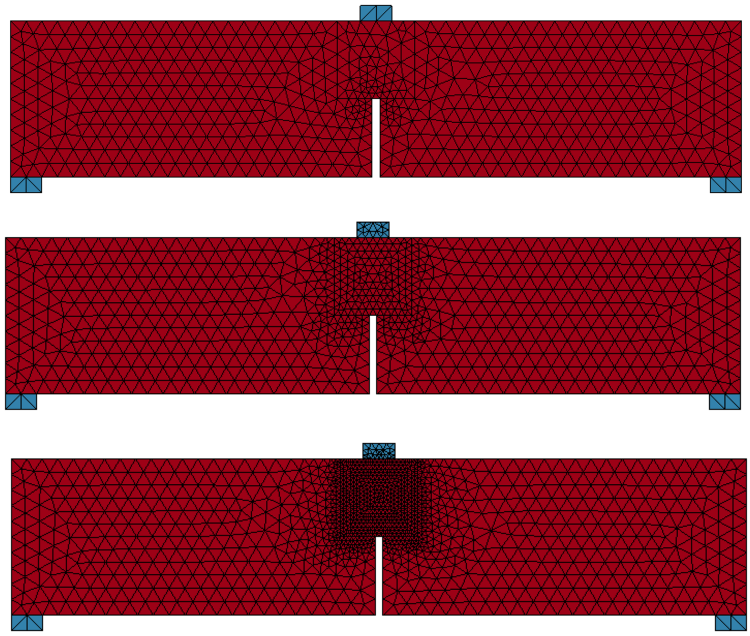

(a)

(b)

(c)

Figure 3: Three point bending test: Coarse, medium and fine tetrahedral meshes.

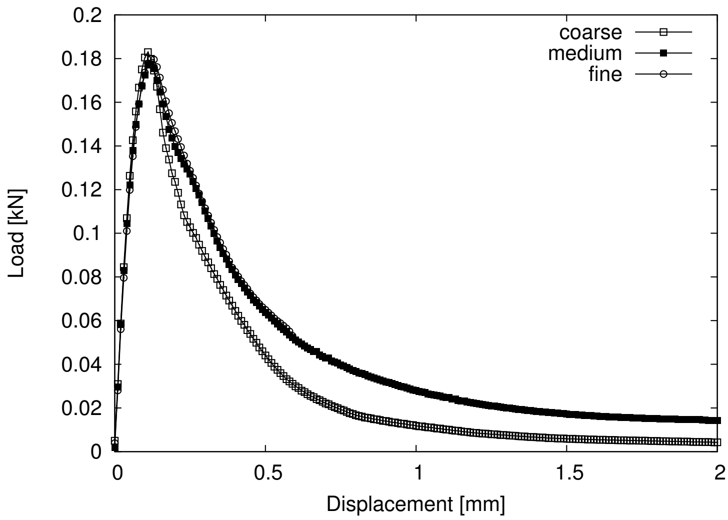

Figure 4: Load versus displacement for three tetrahedral meshes using MAT_CDPM together with the explicit analysis.

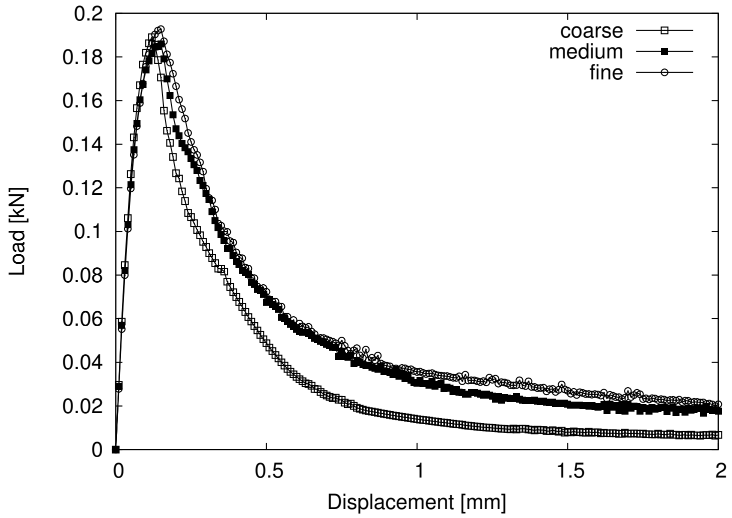

Figure 5: Load versus displacement for three tetrahedral meshes using MAT_CDPM together with the implicit analysis.

analyses are very slow because of the small time steps required for the fine meshes. For the fine mesh, the analysis was stopped earlier than for the medium and coarse mesh because of this slow progress. The same analyses were also the performed with the implicit version of LS-DYNA which were completed much faster. The input files are located in the folders TetraCoarseImplicit, TetraMediumImplicit and TetraFineImplicit. The load-displacement curves for the three implicit analyses are shown in Figure 5. The results of both the explicit and implicit analyses show that the responses for the medium and fine meshes are very similar. Only the coarse meshes produce a steeper softening response. There is not much difference between the load-displacement curves obtained from the explicit and implicit analyses, except that the implicit analyses produce slightly higher load capacities than the explicit analyses and a less smooth post-peak response, which could be improved by setting a stricter tolerance in the implicit analyses. The analysis times of the implicit analyses were significantly smaller than the explicit analyses.

Furthermore, the three-point bending test was also analysed with hexahedral meshes using the explicit version of LS-DYNA. The input files for the analyses are located in the folders HexCoarse, HexMedium and HexFine. The meshes are shown in 6. Again,

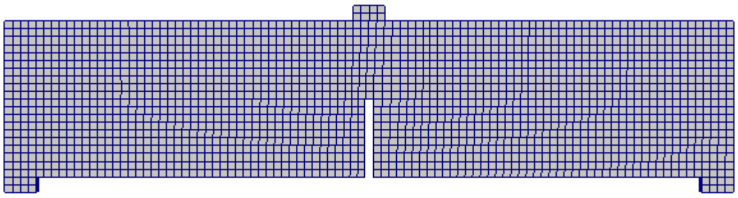

(a)

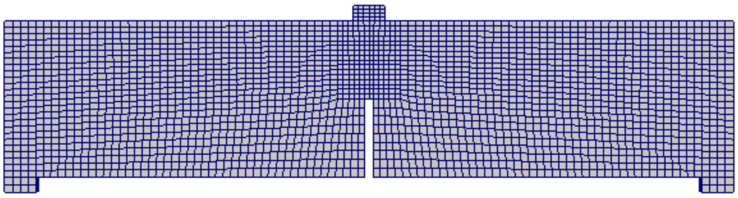

(b)

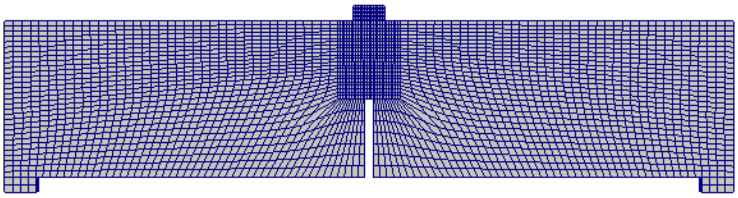

(c)

Figure 6: Three point bending test: Coarse, medium and fine hexahedral meshes.

the out-of-plane thickness was set to 0.01 m. The load-displacement curves for these meshes are shown in 7. Also for the hexahedral meshes the load-displacement curves are mesh independent. Comparing the results obtained with the hexahedral and tetrahedral meshes, one can see that the peak loads obtained with the tetrahedral meshes are larger than for the hexahedral meshes. A comparison of the load-displacement curves for the coarse meshes are shown in Figure 8. This difference is explain by the the way how the element length in LS-DYNA is calculated for the different element types. Comparing the stress-displacement curves of a single brick and truss element reveals that the dissipated energy in the triangle element is overestimated, as shown in Figure 10. Reducing the input parameter w_{f} accordingly for the triangular mesh provides a better agreement with the hexahedral and experimental results. In the future, the way how the element length is calculated in LS-DYNA should be changed, so that for both mesh types the same w_{f} can be given. However, for now this problem can be resolved by reducing the threshold so that the threshold used for tetrahedral elements is approximately 56% of the original threshold calculated from the fracture energy. The modified input card is shown in Figure 9.

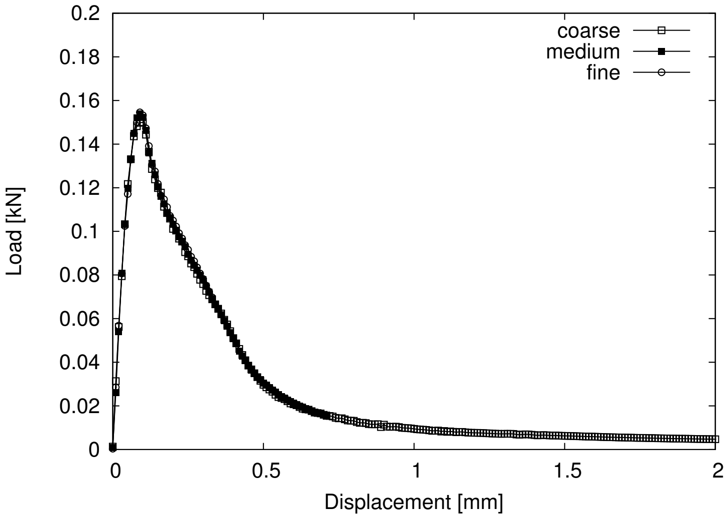

Figure 7: Load versus displacement for three hexahedral meshes using MAT_CDPM together with the explicit analysis.

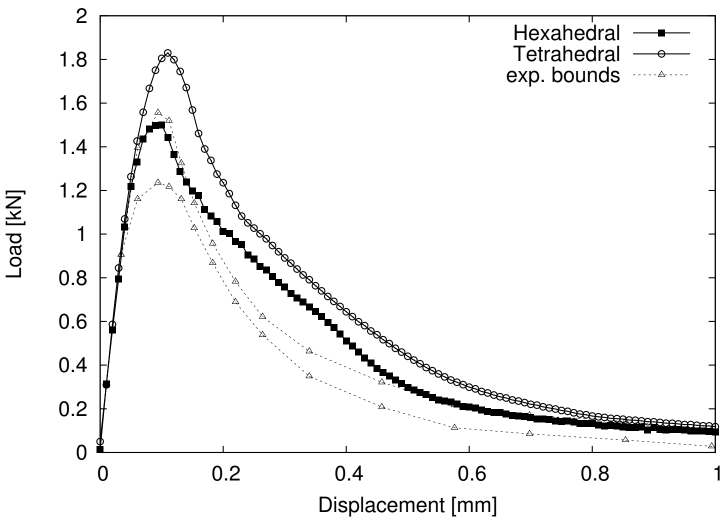

Figure 8: Comparison of Load-displacement curves for the coarse hexahedral and tetrahedral meshes using MAT_CDPM together with the explicit analysis.

```
*MAT_CDPM
$---+----1----+----2----+----3----+----4----+----5----+----6----+----7----+----8
$        |         |         |         |         |         |         |         |
$      MID       RHO         E        PR       ECC       QH0        FT        FC
         1    2.30E3     20.E9                                   2.4e6     24.e6
$        |         |         |         |         |         |         |         |
$       HP        AH        BH        CH        DH        AS        DF       FC0
     0.01                                                   10
$        |         |         |         |         |         |         |         |
$     TYPE        BS        WF       WF1       FT1    STRFLG   FAILFLG       EFC
        1            106.24e-6
```

Figure 9: Modified input card for the three-point bending test with tetrahedral meshes.

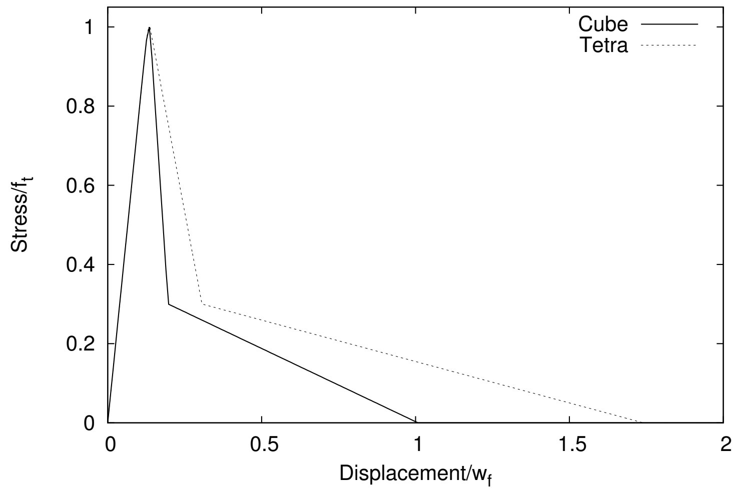

Figure 10: Comparison of Stress-displacement curves for a single brick and tetrahedron using MAT_CDPM together with the explicit analysis.

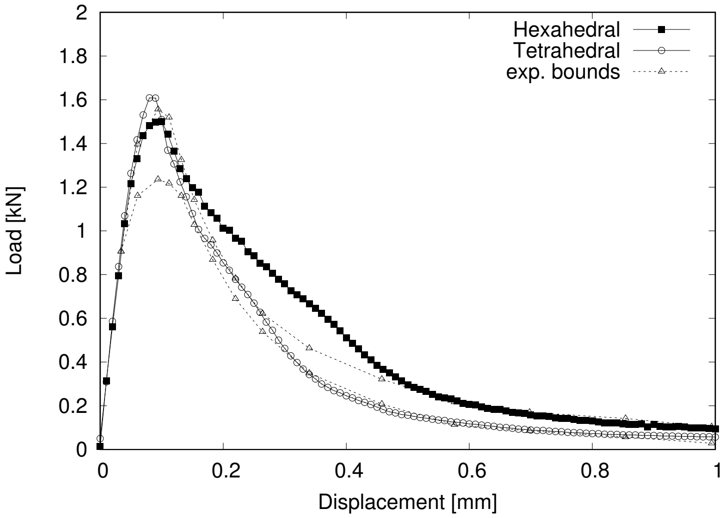

Figure 11: Comparison of Load-displacement curves for the coarse hexahedral and tetrahedral meshes using MAT_CDPM with the modified input for the tetrahedral mesh using the explicit analysis technique.

The load-displacement curve for the coarse tetrahedral mesh with the adjusted threshold was compared with the hexahedral and experimental results in Figure 11. For adjusted threshold, the peak of the load-displacement curve is very similar to the one of the hexahedral mesh.

References

Grassl, P., Jirásek, M., 2006. Damage-plastic model for concrete failure. International Journal of Solids and Structures 43, 7166–7196.

Grassl, P., Nyström, U., Rempling, R., Gylltoft, K., 2011. A damage-plasticity model for the dynamic failure of concrete, in: 8th International Conference on Structural Dynamics, Leuven, Belgium.

Grassl, P., Xenos, D., Nyström, U., Rempling, R., Gylltoft, K., 2013. CDPM2: A damage-plasticity approach to modelling the failure of concrete. International Journal of Solids and Structures 50, 3805–3816.

Kormeling, H.A., Reinhardt, H.W., 1982. Determination of the fracture energy of normal concrete and epoxy-modified concrete. Stevin Laboratory 5-83-18. Delft University of Technology.

Rypl, D., 1998. Sequential and Parallel Generation of Unstructured 3D Meshes. Ph.D. thesis. Czech Technical University. Prague, Czech Republic.